

**Digit replacement dynamics:  
From fixed points and oscillations  
to strange non-chaotic attractors  
and fractal surface growth**

Vladimir García-Morales<sup>1</sup>

<sup>1</sup>*Departament de Termodinàmica, Universitat de València, E-46100 Burjassot, Spain\**

Abstract

A simple nonlinear map is formulated as a toy model for a wide variety of dynamical behavior found in physical systems. The dynamics of the map is elucidated in detail and admits exact solutions for wide regions in parameter space. The mathematical method employed (digit manipulation) opens a new pathway to get insight in complex phenomena such as oscillations with complex waveforms, the emergence of different basins of attraction in phase space with different qualitative properties, and the phenomenon of aperiodic non-chaotic oscillations. The simplicity of the map allows for detailed treatment and for the explicit mathematical design (or modeling) of complex dynamical systems. As an application, we construct a model for deterministic hierarchical deposition of grains of different sizes on a surface, the map being shown to display exotic fractal surfaces as attractors.

PACS numbers: 02.70.Bf, 05.45.Ac, 05.45.Df

---

\*Electronic address: garmovla@uv.es

## I. INTRODUCTION

First-order difference equations arise in many different scenarios in the physical and social sciences [1]. Already deterministic models with just one degree of freedom, as the logistic map, can exhibit a wide variety of dynamical behavior from periodic oscillations to bifurcations into chaos. In spite of the simplicity of their formulation, the dynamics is very complicated and subtle [2, 3], and the understanding of its major implications (and applications) have occupied the efforts of many scientists of different disciplines in the last four decades.

In this article we study a class of first-order difference equations which involve only one degree of freedom as well, but for which the nonlinearity is made tractable so that we can know beforehand whether the system will display aperiodic dynamics or will converge to a fixed point and/or a limit cycle before actually performing any computation. Furthermore, we find that the shape of the oscillations on the limit cycle can be mathematically engineered, as it is the case of some detailed features of the attractors as well. We illustrate these statements by designing an explicit toy model for strange non-chaotic attractors [4, 5] in which, although the trajectory is aperiodic, it is not exponentially sensitive to initial conditions. The class of equations treated here are *not* polynomials of the dynamical variable  $x_t$  but are always specific instances of the following general form

$$x_{t+1} = x_t + g(x_t, t; m, n, p, \mu)p^{f(x_t, t; m, p, \mu)} \quad (1)$$

where  $x_t$  and  $x_{t+1}$  are non-negative real numbers, representing, e.g. the concentration of a chemical species at discrete times  $t$  and  $t + 1$ . The parameter  $p$ , that we shall call the *radix* for reasons that shall soon be obvious, is a natural number  $p \geq 2$ . Parameters  $m$  and  $n$  are natural numbers as well. The fourth and last parameter  $\mu$  is a non-negative real number instead. The function  $g(x_t, t; m, n, p, \mu)$  is an integer in the closed interval  $[-p + 1, p - 1]$ . Finally, the function  $f(x_t, t; m, p, \mu)$  can take any integer value. Because of these definitions, it is clear that the term  $g(x_t, t; m, n, p, \mu)p^{f(x_t, t; m, p, \mu)}$  is a rational number. We shall make explicit the form of the functions  $f(x_t, t; m, p, \mu)$  and  $g(x_t, t; m, n, p, \mu)$  once we have introduced the replacement operator. The dynamics provided by Eq. (1) is thus a first order difference equation where  $x_{t+1} - x_t$  is always a rational number which, as we shall see, only changes one digit of  $x_t$  when  $x_t$  is written in radix  $p$ . In this way, the instantaneous change of  $x_t$  at any time step takes place on a specific scale that is sharply separated from all

others, which remain unaffected. This leads one to be able to tackle the nonlinear behavior of Eq. (1) and no bifurcation diagram needs to be calculated to understand the dynamics in the whole parameter space spanned by the four parameters  $m, n, p$  and  $\mu$ .

A physical application that motivates the introduction of this class of difference equations is the problem of hierarchical deposition of debris on a surface, in which grains of different sizes are deposited in an order related to their size, from larger to smaller grains [6–9]. We propose a simple map for deterministic hierarchical deposition on a surface and show how the fractal surfaces that we have recently constructed in [10] arise as attractors of its dynamical evolution. The model can also be adapted to other instances of fractal surface growth [11, 12].

This article is organized as follows. In Section II we briefly introduce the main mathematical tools, the digit function and the replacement operator, in which our approach is based. Then in Section III we present a general map of the form of Eq. (1) that we term the *digital map* and proceed to dissect its dynamical behavior for different parameter values. In Section IV we formulate a model of deterministic hierarchical deposition on a surface and we conclude with some considerations on the digit function of spatial patterns.

## II. THE DIGIT FUNCTION AND THE REPLACEMENT OPERATOR

Let  $p$  be a natural number  $> 1$ . A non-negative real number  $x$  can be represented in radix  $p$  as [13]

$$x = \sum_{k=-\infty}^{\lfloor \log_p x \rfloor} p^k \mathbf{d}_p(k, x) \quad (2)$$

where  $\mathbf{d}_p(k, x)$  is the digit function, defined as [13]

$$\mathbf{d}_p(k, x) = \left\lfloor \frac{x}{p^k} \right\rfloor - p \left\lfloor \frac{x}{p^{k+1}} \right\rfloor \quad (3)$$

where the brackets  $\lfloor \dots \rfloor$  denote the floor (lower closest integer) function. As an example, in the decimal radix  $p = 10$ , the number  $\pi \equiv 3.1415\dots$  has digits  $\mathbf{d}_{10}(0, \pi) = 3$ ,  $\mathbf{d}_{10}(-1, \pi) = 1$ ,  $\mathbf{d}_{10}(-2, \pi) = 4$ ,  $\mathbf{d}_{10}(-3, \pi) = 1$ ,  $\mathbf{d}_{10}(-4, \pi) = 5$  etc.

In this paper we shall consider  $t$  a non-negative integer. In this case  $\mathbf{d}_p(0, t) = t \bmod p$ , i.e. the zeroth digit function of an integer number is equal to that number modulo the radix

$p$ . We observe that for  $t$  a non-negative integer

$$\mathbf{d}_1(0, t) = 0 \quad (4)$$

$$\mathbf{d}_\infty(0, t) = t \quad (5)$$

The number  $\lfloor \log_p x \rfloor$  in Eq. (2) is the maximum exponent of the power of the radix with which  $x$  is represented in radix  $p$  [14]. Thus the quantity  $p^{\lfloor \log_p x \rfloor}$  gives the *order of magnitude* of  $x$ .

Trivial properties of the digit function that can be directly checked from its definition are the  $p^{k+1}$  periodicity

$$\mathbf{d}_p(k, x + p^{k+1}) = \mathbf{d}_p(k, x) \quad (6)$$

and the scaling invariance

$$\mathbf{d}_p(k, x) = \mathbf{d}_p(0, p^{-k}x) \quad (7)$$

The reader is referred to [13] for other properties of the digit function and a detailed discussion/derivation of them.

We define the replacement operator,  $\mathcal{R}_p(j, k; a, b)$  as

$$\mathcal{R}_p(j, k; a, b) \equiv a + \text{sign}(a)p^j (\mathbf{d}_p(k, |b|) - \mathbf{d}_p(j, |a|)) \quad (8)$$

This operator replaces the  $j$ -th digit of  $a$  (when written in radix  $p$ ) by the  $k$ -th digit of  $b$ .

We observe that, for any integers  $h$  and  $j$ , the following important relationship holds

$$\mathcal{R}_p(h + j, i + k; p^h a, p^i b) = p^h \mathcal{R}_p(j, k; a, b) \quad (9)$$

### III. THE DIGITAL MAP AND ITS DYNAMICAL BEHAVIOR

In this paper we study the dynamics of the map

$$x_{t+1} = \mathcal{R}_p(\lfloor \log_p x_t \rfloor - \mathbf{d}_m(0, t), \lfloor \log_p \mu \rfloor - \mathbf{d}_n(0, t); x_t, \mu) \quad (10)$$

where  $m$  and  $n$  are natural numbers or arbitrary natural-valued functions of  $x_t$ ,  $\mu$  and/or  $t$ . For simplicity, we shall take  $x_t$  to denote non-negative real numbers (denoting e.g. the concentration of some chemical species). Time  $t$  is a non-negative integer. The map generally depends thus on four parameters  $p \geq 2$ ,  $m$  and  $n$  being natural numbers and  $\mu$  a non-negative

real number. We thus see that Eq. (10) is a specific case of Eq. (1) since, from Eqs. (8) and (10) we have

$$\begin{aligned} g(x_t, t; m, n, p, \mu) &\equiv \mathbf{d}_p(\lfloor \log_p \mu \rfloor - \mathbf{d}_n(0, t), \mu) - \mathbf{d}_p(\lfloor \log_p x_t \rfloor - \mathbf{d}_m(0, t), x_t) \\ f(x_t, t; m, p, \mu) &\equiv \lfloor \log_p x_t \rfloor - \mathbf{d}_m(0, t) \end{aligned} \quad (11)$$

The richness of the dynamical behavior of Eq. (10) is better explored step by step by considering specific values for the parameters. If  $m = n = 1$ , Eq. (10) reduces to

$$x_{t+1} = \mathcal{R}_p(\lfloor \log_p x_t \rfloor, \lfloor \log_p \mu \rfloor; x_t, \mu) \quad (12)$$

which trivially replaces the most significant digit of  $x_t$  by the one of  $\mu$  and does nothing else. Thus, already on the first time step, a first point  $x_\infty$  is so reached, with value

$$x_\infty = x_1 = \mathcal{R}_p(\lfloor \log_p x_0 \rfloor, \lfloor \log_p \mu \rfloor; x_0, \mu) \quad (13)$$

In the following, we shall consider increasingly complex dynamics.

### A. Relaxation to a fixed point ( $m = n = \infty$ )

Let  $m = n = \infty$ . In this case, by using Eq. (5), Eq. (10) reduces to the simple form

$$x_{t+1} = \mathcal{R}_p(\lfloor \log_p x_t \rfloor - t, \lfloor \log_p \mu \rfloor - t; x_t, \mu) \quad (14)$$

which can be exactly solved for any initial condition  $x_0$  as

$$x_t = \sum_{j=-\lfloor \log_p x_0 \rfloor}^{t-1-\lfloor \log_p x_0 \rfloor} p^{-j} \mathbf{d}_p(\lfloor \log_p \mu \rfloor - \lfloor \log_p x_0 \rfloor - j, \mu) + \sum_{j=t-\lfloor \log_p x_0 \rfloor}^{\infty} p^{-j} \mathbf{d}_p(-j, x_0) \quad (15)$$

The proof of this result is trivial by induction. At  $t = 0$  we have

$$x_{t=0} = \sum_{j=-\lfloor \log_p x_0 \rfloor}^{\infty} p^{-j} \mathbf{d}_p(-j, x_0) = x_0 \quad (16)$$

Let us assume Eq. (15) valid at time  $t$ . Then, at time  $t + 1$

$$x_{t+1} = \mathcal{R}_p(\lfloor \log_p x_t \rfloor - t, \lfloor \log_p \mu \rfloor - t; x_t, \mu)$$

$$\begin{aligned}
&= \sum_{j=-\lfloor \log_p x_0 \rfloor}^{t-1-\lfloor \log_p x_0 \rfloor} p^{-j} \mathbf{d}_p(\lfloor \log_p \mu \rfloor - \lfloor \log_p x_0 \rfloor - j, \mu) + \sum_{j=t-\lfloor \log_p x_0 \rfloor}^{\infty} p^{-j} \mathbf{d}_p(-j, x_0) + \\
&\quad + p^{\lfloor \log_p x_t \rfloor - t} (\mathbf{d}_p(\lfloor \log_p \mu \rfloor - t, \mu) - \mathbf{d}_p(\lfloor \log_p x_t \rfloor - t, x_0)) \\
&= \sum_{j=-\lfloor \log_p x_0 \rfloor}^{t-\lfloor \log_p x_0 \rfloor} p^{-j} \mathbf{d}_p(\lfloor \log_p \mu \rfloor - \lfloor \log_p x_0 \rfloor - j, \mu) + \sum_{j=t+1-\lfloor \log_p x_0 \rfloor}^{\infty} p^{-j} \mathbf{d}_p(-j, x_0) \quad (17)
\end{aligned}$$

where we have used the obvious fact that, in this case  $\lfloor \log_p x_t \rfloor = \lfloor \log_p x_0 \rfloor \forall t$ . This proves the validity of Eq. (15). Thus, the map converges to the fixed point

$$x_\infty = \sum_{j=-\lfloor \log_p x_0 \rfloor}^{\infty} p^{-j} \mathbf{d}_p(\lfloor \log_p \mu \rfloor - \lfloor \log_p x_0 \rfloor - j, \mu) = \mu p^{\lfloor \log_p x_0 \rfloor - \lfloor \log_p \mu \rfloor} \quad (18)$$

We observe that there is indeed an infinite number of isolated fixed points separated in value by powers of  $p$ . The fixed point  $x_\infty = \mu$  is always present regardless of the value of  $p$ , although its basin of attraction (which corresponds to all those initial conditions for which  $\lfloor \log_p x_0 \rfloor = \lfloor \log_p \mu \rfloor$ ) is explicitly  $p$ -dependent. Thus, if  $x_\infty$  is the fixed point corresponding to  $x_0$ ,  $x_\infty$  attracts all initial conditions in the semiopen interval  $[p^{\lfloor \log_p x_0 \rfloor}, p^{\lfloor \log_p x_0 \rfloor + 1})$  but there is also a fixed point  $p^n x_\infty$  for any  $n \in \mathbb{Z}$  which attracts all initial conditions in the interval  $[p^{n+\lfloor \log_p x_0 \rfloor}, p^{n+\lfloor \log_p x_0 \rfloor + 1})$ . *The existence of these fixed points is a consequence of the scale invariance implied by Eq. (9).* From Eq. (18) we also observe that *the larger  $p$ , the wider the basins of attractions of the fixed points.* We also note that for  $x_0 = 0$ ,  $x_\infty = 0$  independently of  $\mu$  since  $\lfloor \log_p 0 \rfloor = -\infty$ .

In Fig. 1 the evolution of  $x_t$  is plotted for initial conditions  $x_0 \in [1, 9900]$  as obtained from Eq. (15) for  $\mu = \pi$  and for  $p = 2$  (left) and  $p = 10$  (right). We observe the existence of fixed points for the values predicted by Eq. (18) and the observation made above that the larger  $p$ , the wider their basins of attraction. In the range of initial conditions considered, there are 13 fixed points for  $p = 2$  and four fixed points for  $p = 10$ . As we see, independently of the value of  $p$ ,  $\mu = \pi$  is always a fixed point for the range of initial conditions  $\lfloor \log_p x_0 \rfloor = \lfloor \log_p \mu \rfloor$  (the thickness of the basin of attraction of the fixed point being  $p$ -dependent) as obtained from the theory above. We also observe that the smaller  $p$ , the slower the convergence to the fixed points. This is clear from the fact that for lower  $p$  and constant  $x_0$ , more digits are needed to render  $x_0$  up to a certain precision and the number of such significant digits is directly proportional to the duration of the transient. The evolution to  $\mu$ , starting from an

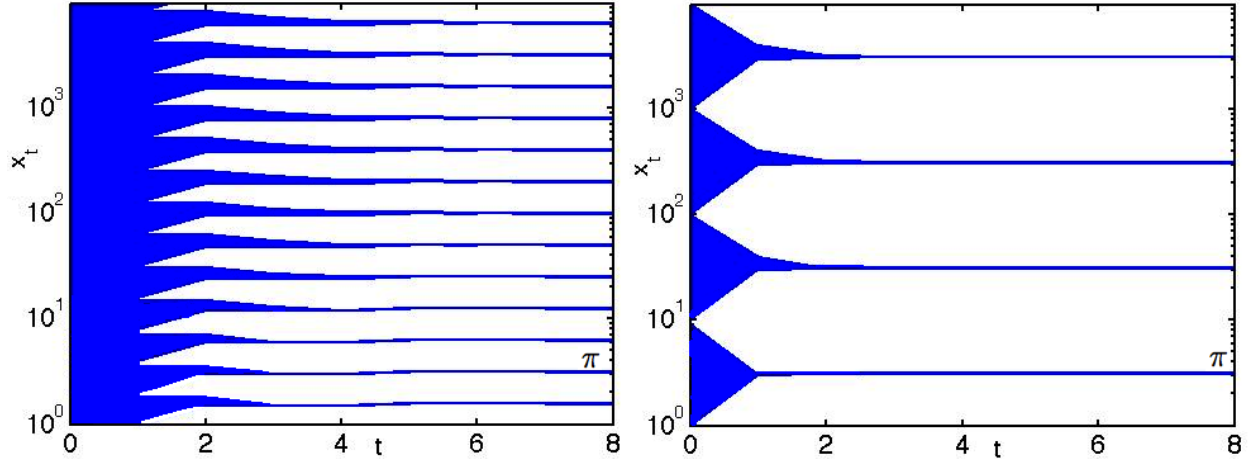


FIG. 1: First eight iterates of the map Eq. (14) for  $\mu = \pi$  starting from initial conditions  $x_0 \in [1, 9900]$  and for  $p = 2$  (left) and  $p = 10$  (right). The fixed point at  $\mu (= \pi$  in this case) is always present, independently of the value of  $p$ , although its basin of attraction is wider for  $p$  larger. Note the logarithmic scale on the  $x_t$  axis.

arbitrary  $x_0$  generally converges in a non-monotonic, nonlinear manner. For  $x_0 = \sqrt{2}$  the successive iterates of the map for  $\mu = \pi$  and  $p = 10$  are

$$\begin{aligned}
 x_0 &= 1.414213\dots & x_1 &= \mathbf{3.4}14213\dots & x_2 &= \mathbf{3.11}4213\dots \\
 x_3 &= \mathbf{3.144}213\dots & x_4 &= \mathbf{3.141}213\dots & x_5 &= \mathbf{3.14151}3\dots & \dots & x_\infty &= \pi
 \end{aligned}$$

where it is clear that the convergence to the fixed point  $\pi$  is achieved by replacing at each time step  $t$  a less significant digit of  $x_0$  by the corresponding one of  $\pi$  (the digits that have been replaced are written in bold above). For  $p = 2$ , we have, however, the sequence of iterates given by

$$\begin{aligned}
 x_0 &= 1.414213\dots & x_1 &= 1.914213\dots & x_2 &= 1.664213\dots \\
 x_3 &= 1.539213\dots & x_4 &= 1.601713\dots & x_5 &= 1.570463\dots & \dots & x_\infty &= \pi/2
 \end{aligned}$$

as predicted by the above development. Although this latter evolution may seem more difficult to grasp, it becomes at once clear when we write these same numbers in the binary radix. Then we observe that the dynamics proceeds by gradually replacing the digits of  $x_0$  by those of  $\mu$  (from the most to the less significant digits). Although, of course, the resulting numbers are the same in any radix, the radix  $p$  offers the best *representation* [15] of the dynamics that is taking place when we tune  $p$  in Eq. (10).

If  $m = \infty$ , but  $n$  is finite, Eq. (10) reduces to

$$x_{t+1} = \mathcal{R}_p \left( \lfloor \log_p x_t \rfloor - t, \lfloor \log_p \mu \rfloor - \mathbf{d}_n(0, t); x_t, \mu \right) \quad (19)$$

In this regime less and less significant digits of  $x_t$  are being replaced by each of the  $n$  most significant digits of  $\mu$ , which are being cyclically chosen (from most to less significant places). In this way, Eq. (19) converges to a fixed point  $x_\infty$  which happens to be a *rational number* such that, when written in radix  $p$ ,  $x_\infty$  has period  $n$  after the radix point (or after the digit  $\lfloor \log_p \mu \rfloor$  if  $\lfloor \log_p \mu \rfloor < 0$ ). Note that, although  $\mu$  can be irrational,  $x_\infty$  contains only the  $n$  most significant digits of  $\mu$  which are periodically repeated after the radix point and arranged on successively decreasing powers of the radix  $p$ .

### B. Periodic orbits ( $m \geq 1, n > 1$ )

We now first consider  $m = 1$  and  $n > 1$  both finite in Eq. (10), which reduces in this case to

$$x_{t+1} = \mathcal{R}_p(\lfloor \log_p x_t \rfloor, \lfloor \log_p \mu \rfloor - \mathbf{d}_n(0, t); x_t, \mu) \quad (20)$$

At each time step the most significant digit of  $x_t$  is replaced by a digit of  $\mu$  that is  $\mathbf{d}_n(0, t)$  digits away (to less significant places) from the most significant digit of  $\mu$ , given by  $\lfloor \log_p \mu \rfloor$ . There are two possibilities: 1) any of the  $n$  most significant digits of  $\mu$  is equal to zero when written in radix  $p$ , in which case  $x_t$  converges to zero; 2) none of the  $n$  most significant digits of  $\mu$  when written in radix  $p$  is zero, in which case, since  $\mathbf{d}_n(0, t)$  has period  $n$ , i.e.  $\mathbf{d}_n(0, t + n) = \mathbf{d}_n(0, t)$ , the orbit of  $x_t$  has period  $n$  as well.

The case 1) is easy to understand. For, if any of the  $n$  most significant digits of  $\mu$  in radix  $p$  is zero, after  $n$  time steps the most significant digit of  $x_t$  is replaced by zero and as a result  $\lfloor \log_p x_t \rfloor$  becomes more negative. If this process is repeated an infinite number of times  $\lfloor \log_p x_t \rfloor = -\infty$  which means that the most significant digit of  $x_t$  accompanies a power  $p^{-\infty}$  of the radix, i.e. that  $x_t$  has converged to zero.

We now concentrate on the more interesting case 2) in which none of the  $n$  most significant digits of  $\mu$  is zero. The orbit can again be trivially solved in this simple case, and has for any  $t \geq 1$  the form

$$x_t = \mathcal{R}_p(\lfloor \log_p x_0 \rfloor, \lfloor \log_p \mu \rfloor - \mathbf{d}_n(0, t - 1); x_0, \mu) + \sum_{j=0}^{\lfloor \log_p x_0 \rfloor - 1} p^{-j} \mathbf{d}_p(-j, x_0) \quad (21)$$

since all time dependence affects only the most significant digit of  $x_t$  accompanying a power  $p^{\lfloor \log_p x_0 \rfloor}$  of the radix and all other digits are left invariant. This time dependence has period

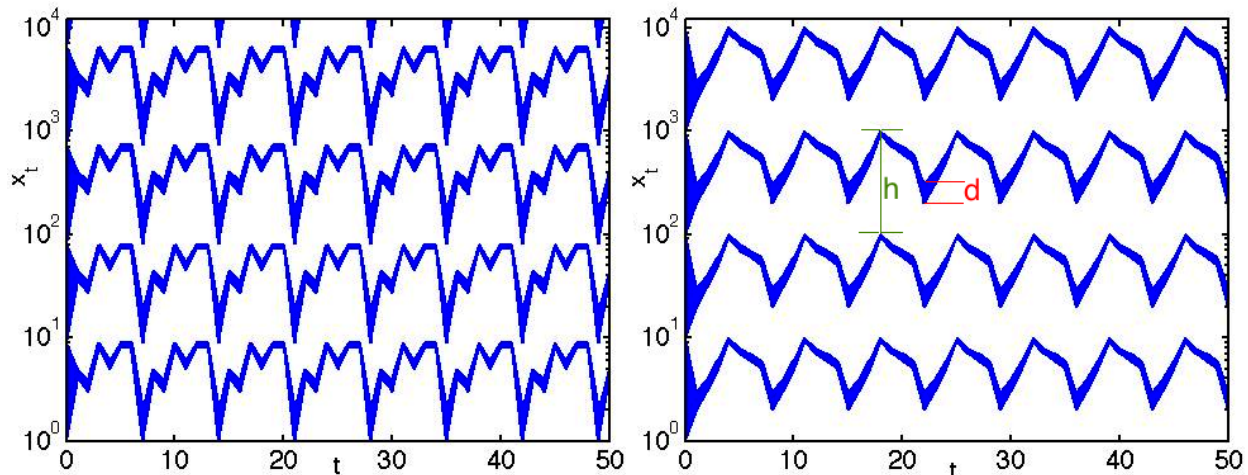


FIG. 2: Evolution of  $x_t$  obtained from the map Eq. (20) for  $p = 9$  (left) and  $p = 10$  (right), for  $\mu = 2359765$  and  $n = 7$ , starting from initial conditions  $x_0 \in [1, 9900]$ . Note the logarithmic scale on the  $x_t$  axis.

$n$  for all  $t > 0$  as can be seen by making the transformation  $t \rightarrow t + n$  and observing that, since  $\mathbf{d}_n(0, t - 1 + n) = \mathbf{d}_n(0, t - 1)$ , this implies, from Eq. (21) that  $x_t = x_{t+n} \forall t \geq 1$ . Thus, for example, for  $b = 27$ ,  $p = 10$  and starting from  $x_0 = \sqrt{2}$ , Eq. (20) produces, for  $p = 10$  the iterates

$$x_0 = 1.41 \dots \quad x_1 = 2.41 \dots \quad x_2 = 7.41 \dots \quad x_3 = 2.41 \dots \quad \dots$$

In Fig. 2, the evolution of the map Eq. (20) is plotted for  $p = 9$  (left) and  $p = 10$  (right), for  $\mu = 2359765$  and  $n = 7$ . In both cases the orbits have period  $T = n = 7$  for all initial conditions. Although the period is the same, the shape of the oscillations is affected by changing  $p$ . Note that for  $p = 10$  the digits of  $\mu = 2359765$  from the most significant to the less significant obey:  $2 < 3 < 5 < 9, 9 > 7 > 6 > 5$ . As a consequence, the shape of the oscillation consist in each period of two different monotonic parts, an increasing one and a decreasing one. For  $p = 9$ , however, since  $\mu = 2359765$  is written as  $\mu = (4385881)_9$  in radix 9, we have that the shape of the oscillation consists of 5 different monotonic parts  $4 > 3, 3 < 8, 8 > 5, 5 < 8 = 8, 8 > 1$ . In both cases we observe the existence of an infinite number of periodic attractors a distance  $h \sim p^{\lfloor \log_p x_0 \rfloor} (p - 1)$  apart, each consisting of a continuous band of periodic orbits which is  $d \sim p^{\lfloor \log_p x_0 \rfloor}$  thick. The existence of such periodic attractors is a consequence of the scale invariance of the replacement operator, made explicit by Eq. (9).

We can now move a step further and consider a more interesting dynamics by taking  $m > 1$  finite as well in Eq. (10). We thus consider Eq. (10) in its full generality. Again, we

have two cases depending on whether any of the  $n$  most significant digits of  $\mu$  in radix  $p$  is zero or not. The outcome of the former case is that  $x_t$  converges to zero for a sufficiently long time, as before. We assume thus the latter case in all what follows. The resulting dynamical evolution depends now on two periods  $n$  and  $m$  which lead, after a transient, to a periodic orbit, where the period  $T = \text{lcm}(m, n)$  is the least common multiple of  $m$  and  $n$ . Note that Eq. (10) is trivially invariant under the transformation  $t \rightarrow t + \text{lcm}(m, n)$ . Again we find attractors with a similar qualitative dynamics albeit with period  $T = \text{lcm}(m, n)$ , as a consequence of the scale invariance, Eq. (9).

Let us now break the above mentioned scale invariance so that the attractors become qualitatively distinct. A simple way of achieving this is to make the dynamics explicitly dependent on the position of the most significant digit of  $x_t$ , i.e. on  $\lfloor \log_p x_t \rfloor$ . Such position sets the most important contribution to the dynamics and corresponds to the order of magnitude of  $x_t$ . Thus, by introducing a dependence of the dynamics on this quantity we explicitly break, by definition, the scale invariance of the dynamics. We thus make  $m$  dependent on  $x_t$  as  $m = 1 + \lfloor \log_p x_t \rfloor$ , i.e., we take  $m$  equal to the number of digits between the most significant digit of  $x_t$  and the first digit to the left of the radix point which is used as reference position. We then note that if  $x_t$  is finite and its evolution is bounded to an interval  $[p^k, p^{k+1})$  then  $m = k$  is constant, and the orbit has periodicity  $\text{lcm}(m, n) = \text{lcm}(k, n)$ . Therefore, since  $m$  depends on  $x_t$  we find that the dynamics now has attractors with different periodicities. We note that, since  $m = 1 + \lfloor \log_p x_t \rfloor = 1$  for any initial condition  $x_0 \in [1, p)$ , Eq. (10) reduces to Eq. (20). The thickness  $d$  calculated previously (see Fig. 2) is now equal to  $d \sim p^{\lfloor \log_p x_0 \rfloor - m + 1} = 1$ .

In Fig. 3 the evolution of  $x_t$  as obtained from Eq. (10) for  $p = 9$  (left) and  $p = 10$  (right), for  $\mu = 2359765$ ,  $n = 7$  and  $m = 1 + \lfloor \log_p x_t \rfloor$  is shown. Besides the oscillations of period  $T = 7$  for initial conditions  $x_0 \in [1, p)$ , which are similar to those in Fig. 2, oscillations with different periodicities  $T = 14, 21, 28$ , are now found for sets of initial conditions  $x_0 \in [p, p^2)$ ,  $x_0 \in [p^2, p^3)$  and  $x_0 \in [p^3, p^4)$ , respectively. Indeed, we have that  $T = \text{lcm}(m, n)$  for the set of initial conditions  $x_0 \in [p^m, p^{m+1})$  and these observed periodicities correspond to the fact that  $m$  is now dependent on the initial condition through  $x_t$ . Different colors have been chosen in Fig. 3 to indicate the now qualitatively different basins of attraction and the behavior of the initial conditions contained in them, thus emphasizing the breaking of the scale invariance. Although the thickness  $d \sim p^{\lfloor \log_p x_0 \rfloor - m + 1} = 1$  is independent of the initial

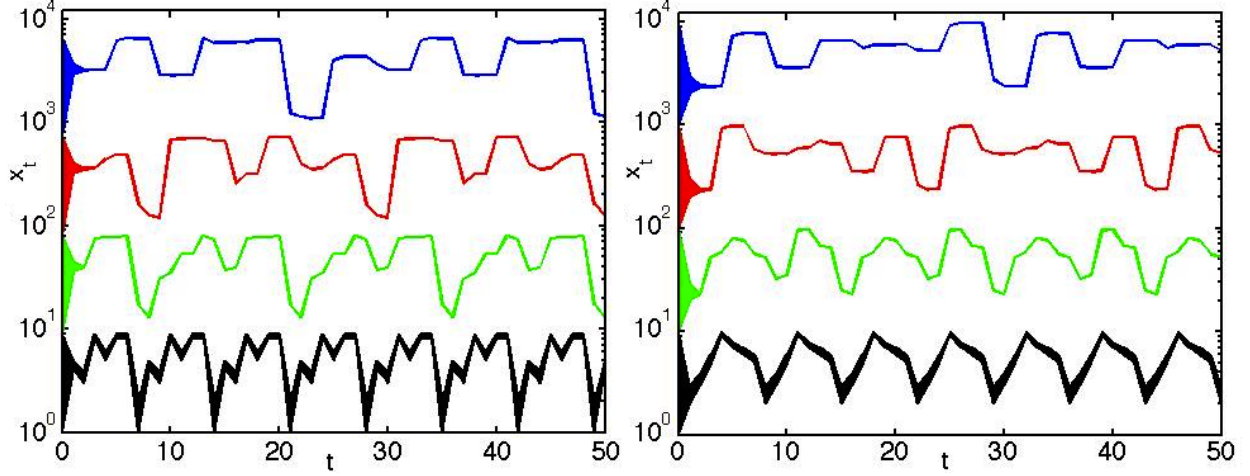


FIG. 3: Temporal evolution of  $x_t$  obtained from the map Eq. (10) for  $p = 9$  (left) and  $p = 10$  (right), for  $\mu = 2359765$ ,  $n = 7$  and  $m = 1 + \lfloor \log_p x_0 \rfloor$ . Note the logarithmic scale on the  $x_t$  axis.

condition, the fact that  $d$  is finite and does no longer scale with  $p^{\lfloor \log_p x_0 \rfloor}$  is revealed in the logarithmic scale of  $x_t$  in Fig. 3 at low powers of the radix.

### C. Aperiodic non-chaotic orbits ( $m \geq 1$ , $n = \infty$ , $\mu \in \mathbb{R}$ irrational)

If  $n = \infty$ , Eq. (10) reduces to

$$x_{t+1} = \mathcal{R}_p(\lfloor \log_p x_t \rfloor - \mathbf{d}_m(0, t), \lfloor \log_p \mu \rfloor - t; x_t, \mu) \quad (22)$$

We now consider the case that  $\mu$  is an irrational number. We have to distinguish two cases: (1) if  $\mu$  has  $N$  digits equal to zero after the radix point when written in radix  $p$ ,  $x_t$  can decay up to a factor  $p^{-N}$  in the course of its trajectory since, each time such a zero is encountered and used to replace the most significant digit of  $x_t$  we have  $\lfloor \log_p x_{t+1} \rfloor = \lfloor \log_p x_t \rfloor - 1$ , i.e. the position of the most significant digit goes to the next less significant place; (2) if  $\mu$  does not contain any digit equal to zero when written in radix  $p$ , we have  $\lfloor \log_p x_t \rfloor = \lfloor \log_p x_0 \rfloor$  i.e., the position of the most significant digit of  $x_t$  is constant, the dynamics is aperiodic and bounded to the interval  $[p^{\lfloor \log_p x_0 \rfloor}, p^{\lfloor \log_p x_0 \rfloor + 1})$  and there exist an infinite number of different aperiodic attractors that are separated and are *not* sensitive to nearby initial conditions. This is easily understood by taking the limit  $n \rightarrow \infty$  from the case discussed above and illustrated in Fig. 3. The period of the oscillations is given by  $T = \text{lcm}(m, n)$  and when  $n$  tends to  $\infty$  so does  $T$ . The dynamics is as follows. The  $m$  most significant digits of  $x_t$  are cyclically replaced by less and less significant digits of  $\mu$ . Therefore, if  $\mu$  is irrational and

does not contain any nonzero digit this process does not end on a finite time and, since less significant digits of  $\mu$  replace the most significant digits of  $x_t$  the temporal evolution of  $x_t$  is necessarily aperiodic.

To find values of  $\mu$  for which no decay to zero happens and one is left with an evolution that is forever aperiodic, let  $\alpha$  be any arbitrary irrational number. Then, the number  $\mu(\alpha)$  defined by

$$\mu(\alpha) \equiv \frac{p^{1+\lfloor \log_p \alpha \rfloor}}{p-1} + \sum_{j=-\infty}^{\lfloor \log_p \alpha \rfloor} \mathbf{d}_{p-1}(j, \alpha) p^j \quad (23)$$

is generally irrational as well (for  $p > 2$ ) and does not contain any digit equal to zero when written in radix  $p$ . To see this note that

$$\mu \equiv \frac{p^{1+\lfloor \log_p \alpha \rfloor}}{p-1} + \sum_{j=-\infty}^{\lfloor \log_p \alpha \rfloor} \mathbf{d}_{p-1}(j, \alpha) p^j = \sum_{j=-\infty}^{\lfloor \log_p \alpha \rfloor} (1 + \mathbf{d}_{p-1}(j, \alpha)) p^j = \sum_{j=-\infty}^{\lfloor \log_p \mu \rfloor} \mathbf{d}_p(j, \mu) p^j \quad (24)$$

where we have used that  $\frac{p^{1+\lfloor \log_p \alpha \rfloor}}{p-1} = \sum_{j=-\infty}^{\lfloor \log_p \alpha \rfloor} p^j$ . Thus, we find that  $\mu$  has digits

$$\mathbf{d}_p(j, \mu) = 1 + \mathbf{d}_{p-1}(j, \alpha) \quad j \in (-\infty, \lfloor \log_p \mu \rfloor] \quad (25)$$

and since  $\mathbf{d}_{p-1}(j, \alpha)$  is an integer which obeys  $0 \leq \mathbf{d}_{p-1}(j, \alpha) \leq p-2$  then  $1 \leq \mathbf{d}_p(j, \mu) \leq p-1$ , and, therefore, no digit of  $\mu$  is equal to zero when written in radix  $p$ . *Such value of  $\mu$  leads Eq. (22) to produce an infinite aperiodic sequence of real numbers which is bounded from above and from below.* Such aperiodic sequence is contained in an aperiodic nonchaotic attractor since the distance between neighboring orbits within the attractor is constant. This is typical of quasiperiodic motion and the attractor obtained can be classified as a 'strange nonchaotic attractor' [4, 5].

Let us illustrate all above with a particular example. We focus first on the former case, where  $\mu$  may contain zero digits when written in radix  $p$ . We take  $\mu = \pi$

$$\pi = 3.1415926535897932384626433832795\underline{0}28841971693993751\underline{0}582\underline{0}9749445923\underline{0}78 \dots$$

and we see that for  $p = 10$  there are digits equal to zero accompanying powers of the radix  $10^{-32}$ ,  $10^{-50}$ ,  $10^{-54}$ ,  $10^{-64}$ , etc. Thus, we expect abrupt decays of those trajectories that satisfy  $\mathbf{d}_{1+|\lfloor \log_p x_t \rfloor|}(0, t) = 0$ , at  $t = 32, 50, 54, 64, \dots$

In Figure 4 (left), the evolution of  $x_t$  obtained from Eq. (22) is plotted for the initial conditions in the set  $x_0 = [1, 9900]$ ,  $m = 1 + |\lfloor \log_p x_0 \rfloor|$  and  $\mu = \pi$ . We see that, although

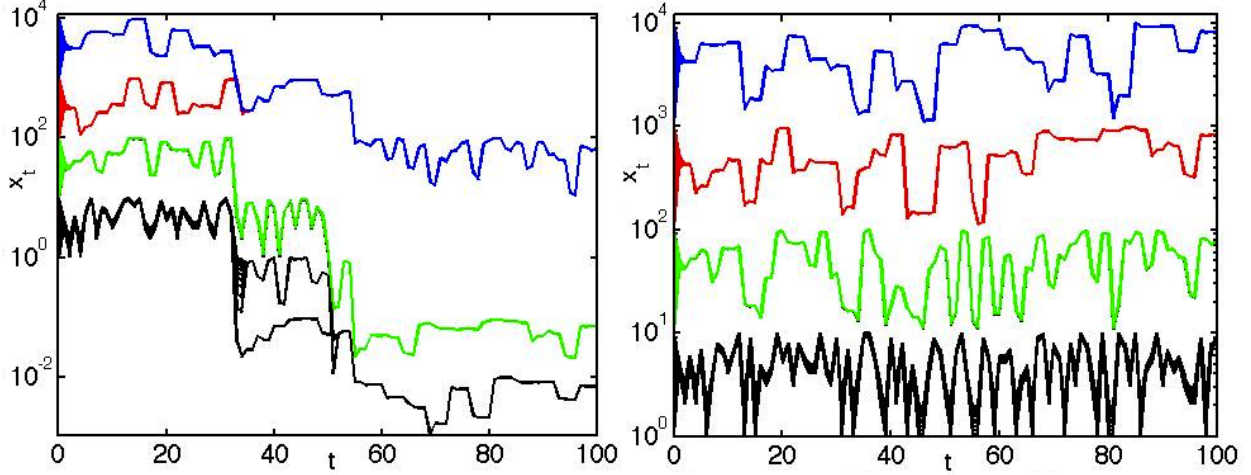


FIG. 4: First 100 iterates of Eq. (22) for  $p = 10$ ,  $m = 1 + \lfloor \log_p x_0 \rfloor$  and  $\mu = \pi$  (left) and  $\mu = \mu(\pi)$  (right), the latter calculated from Eq. (24) for  $\alpha = \pi$  and initial conditions  $x_0 \in [1, 9900]$ .

aperiodic trajectories seem to attract subsets of the initial conditions, some of these trajectories abruptly decay at  $t = 32, 50, 53$  and  $64$  which are those times predicted above. For example, the trajectories colored blue (whose initial conditions belong to the interval  $[10^3, 10^4)$ ) satisfy  $\mathbf{d}_{1+\lfloor \log_p x_t \rfloor}(0, t) = \mathbf{d}_4(0, 32) = 0$  at  $t = 32$  and, therefore, they decay by a factor  $p$  and at  $t = 33$  meet the red curves in the lower level. The latter remain unaffected since they satisfy  $\mathbf{d}_{1+\lfloor \log_p x_t \rfloor}(0, t) = \mathbf{d}_3(0, 32) = 2$ . At a later time, at  $t = 54$  both, blue and red trajectories decay together since now  $\mathbf{d}_{1+\lfloor \log_p x_t \rfloor}(0, t) = \mathbf{d}_3(0, 54) = 0$ . All crossings and complex transitions can thus be explained through the theory presented above. Since  $\pi$  may surely contain an infinite number of digits equal to zero (not regularly spaced), we can safely say that *all trajectories decay to zero after a sufficiently long time*.

Let us now construct an irrational number by means of Eq. (24) such that we can explore the case (2) above in which the trajectories do not decay to zero but  $x_t$  stays bounded within an interval  $\left[ p^{\lfloor \log_p x_0 \rfloor}, p^{\lfloor \log_p x_0 \rfloor + 1} \right)$  forever. From Eq. (24) by taking  $\alpha = \pi$  we find the irrational number

$$\mu(\pi) = 4.2526137646918143495737544943816139952182714114862169311851556134189 \dots \quad (26)$$

which does not contain any zero digit. We now consider the temporal evolution of  $x_t$  taking this latter number  $\mu(\pi)$  as parameter. In Figure 4 (right)  $x_t$  obtained from Eq. (22) is plotted for the initial conditions in the set  $x_0 = [1, 9900]$ ,  $m = 1 + \lfloor \log_p x_0 \rfloor$ ,  $p = 10$  and  $\mu = \mu(\pi)$ . Stable aperiodic oscillations are shown to attract connected sets of initial

conditions. The attractors are all qualitatively distinct, by virtue of the scaling symmetry breaking, and each displays a distinct aperiodic behavior. The trajectory exhibits more abrupt and sudden changes for  $m = 1 + \lfloor \log_p x_0 \rfloor$  close to unity (i.e. for  $x_0 \in [1, p)$ ) and is coarser for  $x_0$  larger. We observe that there is no exponential sensitivity to initial conditions even when the resulting dynamics is forever aperiodic: all close initial conditions within an interval  $[p^{\lfloor \log_p x_0 \rfloor}, p^{\lfloor \log_p x_0 \rfloor + 1})$  are attracted to a thin band of aperiodic trajectories of thickness  $d \sim 1$  where they keep a constant distance.

Although we stop here our discussion of Eq. (10) it should now be clear that if  $\mu$  is no longer a parameter but a function of  $x_t$  as well, we shall have strange chaotic attractors as a result. Already if we simply replace  $\alpha$  by  $x_t$  in Eq. (24) and  $\mu$  by  $\mu(x_t)$  in Eq. (22), the result is an aperiodic dynamics that is exponentially sensitive to initial conditions: The closer two different initial conditions  $x_0$  and  $x'_0$  are, the longer the trajectories evolve together. However, as soon as the corresponding digits of  $x_t$  and  $x'_t$  that are being used to replace the  $m$  most significant digits of  $x_t$  and  $x'_t$  begin to differ, the trajectories begin to depart aperiodically from each other. In the long term, the value of  $x'_t$  cannot be estimated from the value of  $x_t$  even when both  $x_t$  and  $x'_t$  were initially close.

#### IV. SPATIALLY EXTENDED ATTRACTORS: FRACTAL SURFACES, HIERARCHICAL DEPOSITION AND EMERGENCE OF FORM

We can now apply the map Eq. (10) to the following problem of interest to hierarchical deposition processes on a surface in which grains of bigger size deposit first according to a certain rule and a next generation of grains which are smaller by a factor  $\sim 1/p^3$  deposit next. We have recently found [10], that if  $u$  and  $v$  denote spatial coordinates on the plane  $\mathbb{R}^2$  then, for  $R \in [0, p^{p^2} - 1]$  an integer and  $k_{max} \equiv \max\{\lfloor \log_p u \rfloor, \lfloor \log_p v \rfloor\}$ , the function given by

$$\mathbf{b}_p(u, v; R) = \sum_{k=-\infty}^{k_{max}} p^k \mathbf{d}_p(\mathbf{d}_p(k, u) + p\mathbf{d}_p(k, v), R) \quad (27)$$

is a surface with fractal self-affine properties. It is now clear, from the discussion in the preceding section, that such surface will be an attractor of the dynamics given by the map

$$x_{t+1}(u, v) = \mathcal{R}_p(\lfloor \log_p \mathbf{b}_p(u, v; R) \rfloor - t, \lfloor \log_p \mathbf{b}_p(u, v; R) \rfloor - t; x_t(u, v), \mathbf{b}_p(u, v; R)) \quad (28)$$

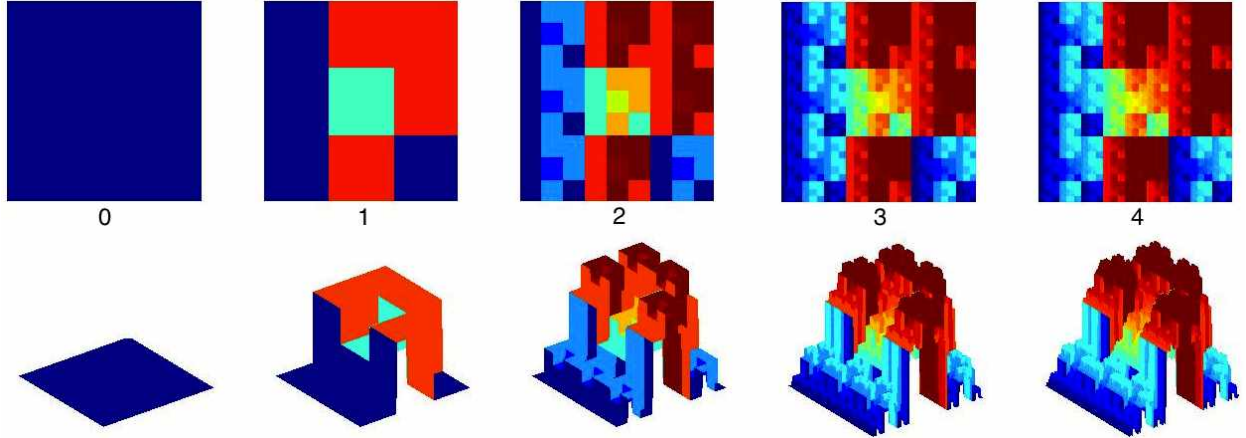


FIG. 5: Four time steps of the spatiotemporal evolution  $x_t(u, v)$  obtained from Eq. (28) for  $p = 3$   $R = 6453$   $u \in [0, 240]$  and  $v \in [0, 240]$ . Two different views of the developing surface are shown, starting from a clean surface at  $t = 0$ .

which corresponds to Eq. (14) with  $\mu = \mathbf{b}_p(u, v; R)$  and with  $x_t$  having now a spatial dependence  $x_t(u, v)$  on the real coordinates  $u$  and  $v$ . By taking into account the results of the previous section, we observe that if we start from a ‘clean’ surface  $x_0(u, v) = 0$  the map shall converge to

$$x_\infty(u, v) = \mathbf{b}_p(u, v; R) \quad (29)$$

for any point  $(u, v)$  on the plane. This convergence proceeds as follows. On the clean surface, in the first iteration the first grains are deposited, with area  $p^{\lfloor \log_p \mathbf{b}_p(u, v; R) \rfloor} \times p^{\lfloor \log_p \mathbf{b}_p(u, v; R) \rfloor}$  and height  $p^{\lfloor \log_p \mathbf{b}_p(u, v; R) \rfloor} \mathbf{d}_p(\mathbf{d}_p(k_{max}, u) + p\mathbf{d}_p(k_{max}, v), R)$ . Then, in the next time step smaller grains with area  $p^{\lfloor \log_p \mathbf{b}_p(u, v; R) \rfloor - 1} \times p^{\lfloor \log_p \mathbf{b}_p(u, v; R) \rfloor - 1}$  and height  $p^{\lfloor \log_p \mathbf{b}_p(u, v; R) \rfloor - 1} \mathbf{d}_p(\mathbf{d}_p(k_{max} - 1, u) + p\mathbf{d}_p(k_{max} - 1, v), R)$  are deposited. The process goes on from the bigger to the smaller scales till convergence to the fractal object  $\mathbf{b}_p(u, v; R)$  is achieved. More significant digits of  $\mathbf{b}_p(u, v; R)$  have a longer spatial variability as we prove in the coarse graining theorem recently reported in [10].

In Figure 5 this process of fractal surface growth is shown for for  $p = 3$   $R = 6453$   $u \in [0, 240]$  and  $v \in [0, 240]$  in Eq. (28). Four time steps of the spatiotemporal evolution  $x_t(u, v)$  are shown, giving at each time step two different views of the same surface. We observe a fractal surface deterministically growing from the coarser to the finer details. Although we have considered a digital replacement dynamics most to less significant digits, it is also possible to select at random the digit to be replaced and the attractor will be the same, after a sufficiently large number of experiments. In combination with our results in [10] this provides an explanation of why iterated functions systems [16] generally lead to

fractal attractors.

The evolution can also proceed from finer to coarser details. Let  $r(u, v)$  be a real-valued function of the coordinates  $u, v$  in the plane. Then, the following dynamics

$$x_{t+1}(u, v) = \mathcal{R}_p(t - D, t - D; x_t(u, v), r(u, v)) \quad (30)$$

gradually replaces the digits of  $x_t(u, v)$  by those of  $r(u, v)$ , starting with the digit accompanying the power  $p^{-D}$  of the radix, and proceeding now from less to more significant digits.

To exemplify this statement, let us consider an arbitrary image encoded in a function  $P(u, v) : \mathbb{R}^2 \rightarrow \mathbb{R}$ . The image colors are all in a gray scale in a one-to-one correspondence with real numbers  $P(u, v) \in [0, 1)$ . We can calculate a truncation of  $P(u, v)$  to  $D$  digits after the radix point by means of the coarse graining operator  $p^{-D} \lfloor p^D \dots \rfloor$  [10]

$$r(u, v) = p^{-D} \lfloor p^D P(u, v) \rfloor \quad (31)$$

A noisy initial condition  $x_0(u, v) \in [0, 1)$  can now be considered as well. Thus, from Eq. (30) it is predicted that the arbitrary noisy initial condition converges to the image  $r(u, v)$  *exactly* after  $D$  discrete time steps starting from the arbitrary (random) initial condition  $x_0(u, v)$ .

In Fig. 6 we observe the evolution of the map Eq. (30) with  $p = 2$  to a target image  $P(u, v)$  taken from the internet, and approximated by  $r(u, v)$  up to  $D = 7$  digits after the radix point by using Eq. (31). We observe that the gradual replacement of more significant digits of  $r(u, v)$  is similar to accounting for features of the target pattern on a longer scale, i.e. the digit function  $\mathbf{d}_p(k, r(u, v))$  has a longer spatial variability for more positive  $k$ , as is the case mentioned above for fractal surfaces and recently reported in [10].

To better understand why the most significant digits of  $r(u, v)$  refer to the coarser structures in an arbitrary pattern with longer spatial variability it is useful to inspect the digit function  $\mathbf{d}_p(k, r(u, v))$  as a function of  $p$  and  $k$ . We have

$$\mathbf{d}_p(k, r(u, v)) = \left\lfloor \frac{r(u, v)}{p^k} \right\rfloor - p \left\lfloor \frac{r(u, v)}{p^{k+1}} \right\rfloor = \left\lfloor p \left\{ \frac{r(u, v)}{p^{k+1}} \right\} \right\rfloor \quad (32)$$

where  $\{\dots\}$  denotes the fractional part. Thus we see that in order for the digit function to change from a value  $\mathbf{d}_p(k, r(u, v))$  to a value  $\mathbf{d}_p(k, r(u, v)) \pm 1$  for certain increments  $\delta_u$  and  $\delta_v$  of the variables  $u$  or  $v$ , we must have

$$|r(u + \delta_u, v + \delta_v) - r(u, v)| \sim p^k$$

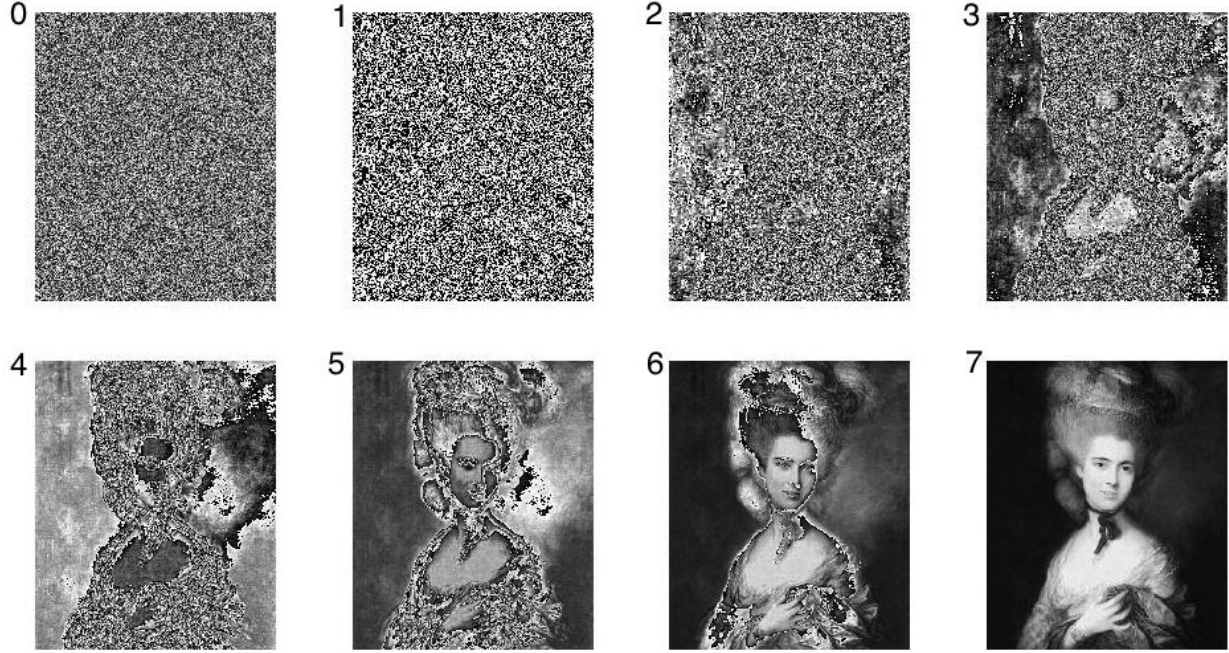


FIG. 6: Spatiotemporal evolution of  $x_t(u, v)$  as provided by the map Eq. (30) starting from a formless, noisy initial condition  $x_0(u, v)$ . Indicated are the values of  $t$  for the iterations of the map, with  $p = 2$  and  $D = 7$  on a matrix of  $520 \times 439$  pixels whose gray tones correspond to real numbers  $\in [0, 1)$ . Convergence of  $x_t(u, v)$  to  $r(u, v)$  is obtained after 7 iterations.

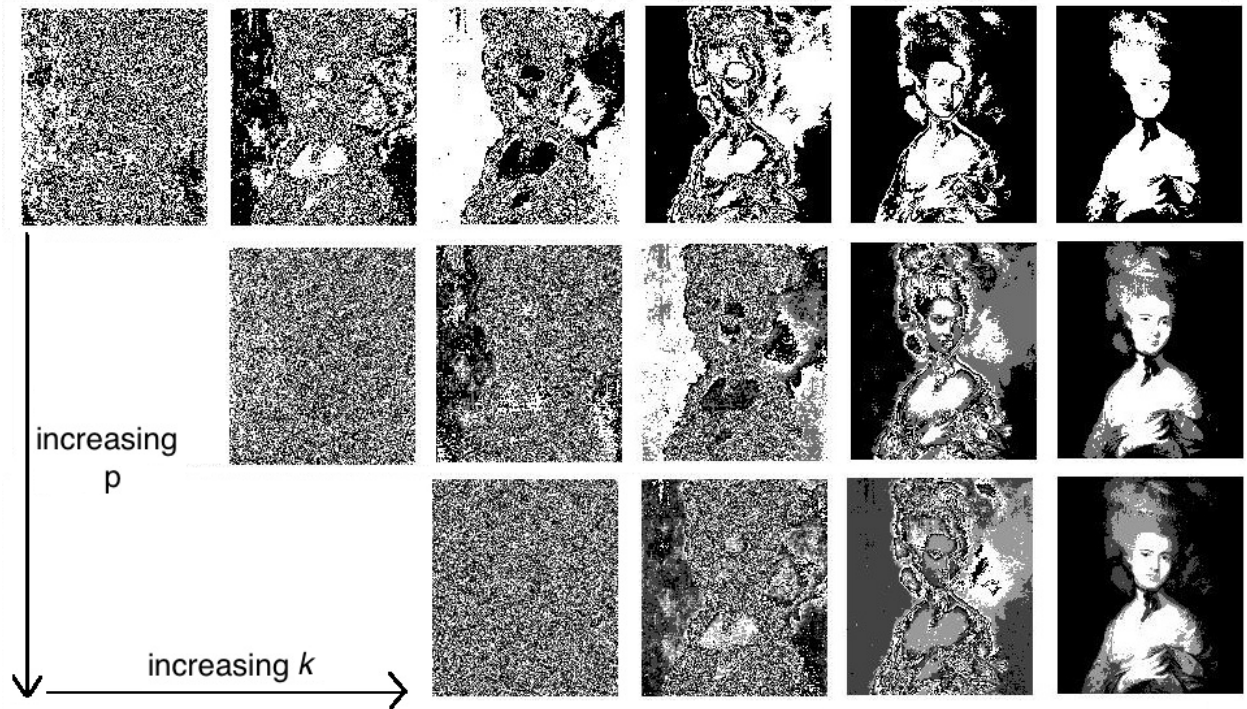


FIG. 7: The function  $\mathbf{d}_p(k, r(u, v))$  for  $r(u, v)$  given by the bottom rightmost panel in Fig. 6 and different values of  $p$  and  $k$  increasing in the directions marked by the arrows in the figure:  $\mathbf{d}_2(-6, r(u, v)), \mathbf{d}_2(-5, r(u, v)), \mathbf{d}_2(-4, r(u, v)), \dots, \mathbf{d}_2(-1, r(u, v))$  (top row);  $\mathbf{d}_3(-5, r(u, v)), \mathbf{d}_3(-4, r(u, v)), \dots, \mathbf{d}_3(-1, r(u, v))$  (middle row) and  $\mathbf{d}_4(-4, r(u, v)), \dots, \mathbf{d}_4(-1, r(u, v))$  (bottom row).

and thus, for larger  $k$ , larger increments  $\delta_u$  and  $\delta_v$  are needed for  $\mathbf{d}_p(k, r(u, v))$  to change in one unit. Of course, this heuristic argument only applies if  $r(u, v)$  is smooth enough. We can explicitly illustrate this simple argument by calculating  $\mathbf{d}_p(k, r(u, v))$  for the pattern  $P(u, v)$  in Fig. 6 for different values of  $k$  and  $p$ . The result is shown in Fig 7 where the following facts are observed: 1) for larger  $p$  and fixed  $k$ ,  $\mathbf{d}_p(k, r(u, v))$  is able to discriminate more structural details and contains more information, as seen in the larger number of tones of gray ; 2) for more positive  $k$  and fixed  $p$  the structures accounted for by  $\mathbf{d}_p(k, r(u, v))$  broadly exhibit a longer spatial variation. Thus, Eq. (30) describes a kind of ‘diffusion process’ (even when it is a purely local model) because it locally incorporates information of longer spatial structures as time progresses, the value of  $x_t(u, v)$  being locally adjusted in a nonlinear, non-monotonic way, to incorporate longer spatial correlations. These remarks can be better understood if we compare our map with the simple differential equation in continuous time provided by

$$\frac{dx}{dt} = r(u, v) - x \quad (33)$$

which has also the fixed point  $x_\infty = r(u, v)$  and trajectory simply given by  $x(t) = r(u, v) - (r(u, v) - x(0))e^{-t}$ . In this case all information contained in  $r(u, v)$  is present at every time both within  $x(t)$  and  $\frac{dx}{dt}$ . This is not the case of our map where the system has only partial information of  $r(u, v)$ . At time  $t$  the system only ‘knows’ of  $r(u, v)$  the layers  $\mathbf{d}_p(k, r(u, v))$  with  $k$  between  $-D$  and  $k = t - D$ . Note that the orbit of Eq. (30) is explicitly given by

$$x_t(u, v) = \sum_{k=0}^{t-1} p^{k-D} \mathbf{d}_p(k - D, r(u, v)) + \sum_{k=t}^{\lfloor \log_p x_0(u, v) \rfloor + D} p^{k-D} \mathbf{d}_p(k - D, x_0(u, v)) \quad (34)$$

and, hence, when  $t \geq \lfloor \log_p r(u, v) \rfloor + D$ , the orbit exactly converges *in a finite time* to the fixed point

$$x_\infty(u, v) = \sum_{k=0}^{\lfloor \log_p r(u, v) \rfloor + D} p^{k-D} \mathbf{d}_p(k - D, r(u, v)) = \sum_{k=-D}^{\lfloor \log_p r(u, v) \rfloor} p^k \mathbf{d}_p(k, r(u, v)) = r(u, v) \quad (35)$$

Thus, all layers of  $r(u, v)$  provided by different  $k$  values of  $\mathbf{d}_p(k - D, r(u, v))$  are separated and independent of each other, each referring to a specific scale. A detailed pattern is formed by superimposing all layers, accompanying them with the scale weight  $p^{k-D}$ . This is thus similar to a kind of anomalous diffusion process, where the system gradually explores all scales through interactions with its neighbors, the neighborhood range increasing with time as well. Indeed, if one stores of any image  $P(u, v)$  the layer corresponding to the

most significant digit  $\mathbf{d}_p([\log_p P(u, v)], P(u, v))$ , one gets a posterized image of  $P(u, v)$  with  $p$  colors (see the rightmost panels of Fig. 7). Thus, by storing also some few layers corresponding to less significant digits (by tuning  $D$ ) one can readily construct  $r(u, v)$  out of  $P(u, v)$  and use Eq. (30) for noise reduction. This model is thus an alternative to edge detection and noise reduction of images as obtained with the Perona-Malik equation [17] and generalized versions of it.

## V. CONCLUSIONS

In this work we have applied digital calculus [10, 13–15] to construct a simple nonlinear map (and variations of it) that operate in discrete time steps by replacing the digits of the numerical value of a dynamical variable  $x_t$  when written in radix (base)  $p$  by those of a control parameter  $\mu$ . We have shown how limit cycle oscillations and aperiodic behavior can be mathematically designed. We have also shown how our toy model leads to a straightforward explanation of strange non-chaotic attractors. Although we have described increasingly complex dynamics, the simplicity of the mathematical approach presented (even when the notation and concepts are unfamiliar) is such that all prominent features displayed by the dynamics could be easily elucidated. We have also applied the methods presented here to construct a simple model for hierarchical deposition on a surface and we have also explained how another variation of the model can be used to model the emergence of form, from the tiniest to the broadest scales.

Although all physical numbers are radix independent, they are all always *represented* in a specific radix (e.g. the usual decimal radix). We have here constructed dynamical systems by regarding the possibility that the digits of the numbers are being replaced at each instant of time (what every function indeed does) one by one. Note that in this article it is *irrelevant* which radix we actually choose for giving the numbers. However, if we choose the radix  $p$  at which the digits are being replaced, it becomes at once clear how the dynamics takes place. Thus, the status of the optimal radix  $p$  (entering here in the replacement operator) compared to any other radix is analogous to the status of a diagonal matrix compared to the same matrix in non-diagonal form. In this latter case we say that Physics is invariant under orthogonal transformations and that it is better to work with a diagonal matrix to understand its action on a vector. In the former case we say that numbers are invariant

under radix change and that it is better to work with the optimal radix to understand the dynamics taking place. In a recent work [15] we have derived physical laws by proposing that the optimal physical radix that constitutes the best representation of the dynamics is the one which has the least economy (i.e. the most efficient radix) and we have related such optimal radix to the floor function of the Lagrangian action.

---

- [1] R. May, *Nature* **261**, 459 (1976).
- [2] M. J. Feigenbaum, *J. Stat. Phys.* **19**, 25 (1978).
- [3] J.-P. Eckmann and D. Ruelle, *Rev. Mod. Phys.* **57**, 617 (1985).
- [4] A. Pikovsky and U. Feudel, *Chaos* **5**, 253 (1995).
- [5] U. Feudel, S. Kuznetsov, and A. Pikovsky, *Strange Nonchaotic Attractors: Dynamics between Order and Chaos in Quasiperiodically Forced Systems* (World Scientific, Singapore, 2006).
- [6] J. O. Indekeu, G. Fleerackers, A. I. Posazhennikova, and E. Bervoets, *Physica A* **285**, 135 (2000).
- [7] A. I. Posazhennikova and J. O. Indekeu, *Int. J. Thermophys.* **22**, 1123 (2001).
- [8] A. I. Posazhennikova and J. O. Indekeu, *Physica A* **414**, 240 (2014).
- [9] A. L. Barabasi and H. E. Stanley, *Fractal concepts in surface growth* (Cambridge University Press, Cambridge, UK, 1995).
- [10] V. García-Morales, *Physica A* **447**, 535 (2016), cs.OH/1507.01444v3.
- [11] T. Vicsek, *Fractal Growth Phenomena* (World Scientific, Singapore, 1989).
- [12] F. Family and T. Vicsek, *J. Phys. A* **18**, L75 (1985).
- [13] V. García-Morales, *Chaos Sol. Fract.* **83**, 27 (2016), cond-mat/1505.02547v3.
- [14] V. García-Morales, *Physica A* **440**, 110 (2015).
- [15] V. García-Morales, *Found. Phys.* **45**, 295 (2015).
- [16] M. F. Barnsley, *Superfractals* (Cambridge University Press, Cambridge, UK, 2006).
- [17] P. Perona and J. Malik, *IEEE Trans. Pattern Anal. Machine Intell.* **12**, 629 (1990).